Noncoherent detection of factor-graph codes over fading channels

R.-R. Chen and D. Agrawal
Coordinated Science Laboratory
University of Illinois at
Urbana-Champaign
Urbana, IL 61801
e-mail: r-chen1@uiuc.edu,
dagrawal@uiuc.edu

U. Madhow[1]
Department of Electrical and
Computer Engineering
University of California
Santa Barbara, CA 93106
e-mail: madhow@ece.ucsb.edu

Abstract — **In this paper, we consider noncoherent multi-symbol detection of factor-graph codes over Rayleigh fading channels. We use block differential encoding together with a joint demodulation and iterative decoding algorithm to eliminate the pilot overhead required for coherent detection. Simulations using turbo codes and repeat-accumulate codes show that as the length of the coherence interval increases, performance of the proposed noncoherent detector approaches that of the coherent detector.**

I. Introduction

Factor-graph codes such as turbo codes are known to perform near channel capacity for both additive white Gaussian noise [1] and Rayleigh fading [2] channels. Much of the work done thus far has been for coherent communication, wherein the channel gain and phase are assumed to be known to the receiver. However, for fast fading channels, the pilot overhead required to estimate the channel gain and phase may be excessive. In this paper, we propose a noncoherent detector for factor-graph codes over fading channels. We assume that the fading is unknown to the receiver, but it remains roughly constant over several symbols. A classical technique employed in this context is differential PSK, where the binary output of the channel encoder is Gray coded and is mapped to a PSK constellation. Resulting PSK symbols are then differentially modulated and transmitted over the fading channel. At the receiver, hard or soft decisions for the transmitted bits are generated using differential demodulation.

In the uncoded case, at high SNR's, the performance of block differential demodulation approaches that of coherent demodulation as the length of the coherence interval gets large [3]. Furthermore, it is shown in [5] that for a block fading channel, the channel capacity approaches that of a coherent channel as the coherence interval gets large. These results indicate that it might be possible to design noncoherent detectors for coded systems whose performance approach that of coherent detectors for analogous systems, and motivate the work undertaken in this paper.

Our main results are as follows:

(a) We employ an overlapped block differential encoder, first proposed in [5]. To the best of our knowledge, overlapped block differential encoding results in a lower decoding complexity compared to the complexity of standard DPSK block demodulation. It's shown that this method effectively provides one pilot symbol per block without incurring any pilot overhead.

(b) We modify the iterative decoding algorithm for factor-graph codes to accommodate block noncoherent demodulation. The modification consists of feeding back soft information from the iterative decoder to the noncoherent demodulator, and thus, doing a 'joint' estimation of channel phase and information bits. The proposed demodulator quantizes channel phase to avoid exponential complexity (in the length of the coherence interval) of the block noncoherent demodulation.

(c) We performed extensive computer simulations to evaluate the performance of the proposed joint demodulation and iterative decoding algorithm. Simulations employing turbo code and repeat-accumulate code show that the performance of the proposed algorithm approaches that of coherent detector as the length of the coherent interval increases.

(d) Simulations show that the decoding algorithm for repeat-accumulate codes converges slower than that of turbo codes. This has a surprising consequence—for small coherence intervals, repeat-accumulate codes outperform turbo codes due to the slow convergence of its decoding algorithm.

A joint demodulation and iterative decoding algorithm, similar to the one presented here, was introduced by Peleg and Shamai for noncoherent detection of convolutional codes over AWGN channels [4]. In a subsequent work, Peleg, Shamai, and Galán [9] extended this noncoherent decoding algorithm to turbo codes over AWGN channels. In other related work, iterative DPSK demodulation based on linear prediction and channel decoding was investigated by Hoeher and Lodge [10].

The remainder of this paper is organized as follows: Section II contains a detailed description of the system model that includes the fading channel, the overlapped block differential encoder and the joint demodulation and iterative decoding algorithm. Section III describes the numerical results. Section IV contains conclusions and discusses directions for the future work.

II. System Model

Figure 1 shows a schematic block diagram of the system. At each time instant, a block of information bits $\{b_i\}$ is input to the channel encoder. The resulting codeword is bit-interleaved and the interleaved bit sequence is mapped to a sequence of PSK symbols using the Gray mapping. Subsequently, the PSK symbols are passed through an overlapped block differential encoder.

[1]This research was supported by the National Science Foundation under a CAREER award NCR96-24008 and by NASA under grant NAG3-2263.

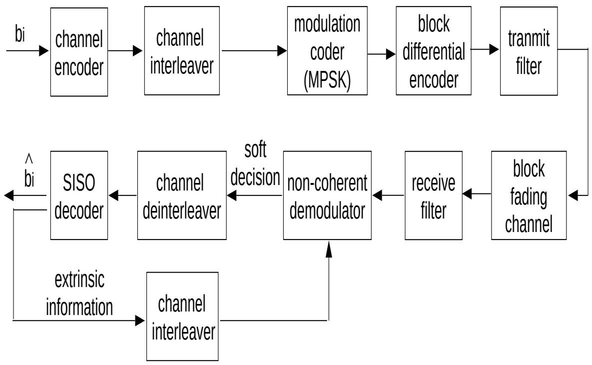

Figure 1: Schematic Block Diagram of the System

A. *Overlapped Block Differential Encoder*

The overlapped block differential encoder takes a block of $N-1$ consecutive PSK symbols $(x_1, x_2, \ldots, x_{N-1})$ and outputs $(x_1 \cdot \hat{x}_{N-1}, x_2 \cdot \hat{x}_{N-1}, \ldots, x_{N-1} \cdot \hat{x}_{N-1})$, where $\hat{x}_{N-1}$ is the last transmitted symbol of the previous block. For example, when $N = 3$, if the input sequence to the overlapped block differential encoder is $(a_0, a_1, a_2, a_3, a_4, a_5, a_6, \cdots)$, then the output of the encoder would be $(a_0, a_1, a_2, a_3 \cdot a_2, a_4 \cdot a_2, a_5 \cdot (a_4 a_2), a_6 \cdot (a_4 a_2), \cdots)$.

B. *Channel Model*

In this paper, we consider a block Rayleigh fading channel. We assume that the fading remain almost constant over a block of N consecutive symbol periods. We assume that the fading is unknown to the receiver.

C. *Block Noncoherent Demodulator*

At the complex baseband receive filter, the output is grouped in overlapping blocks of N samples. For example, when $N = 3$, if the output of the receive filter is $(b_0, b_1, b_2, b_3, b_4, \cdots)$, then the resulting overlapped blocks will be (b_0, b_1, b_2), (b_2, b_3, b_4), (b_4, b_5, b_6), $\cdots$. Since, we assume that the fading remains almost constant over any N consecutive symbol periods, a received block $\mathbf{y} = (y_0, y_1, \ldots, y_{N-1})$ can be modeled as follows:

$$\begin{aligned}\mathbf{y} &= (y_0, y_1, \ldots, y_{N-1}) \\ &= h(\hat{x}_{N-1}, x_1 \cdot \hat{x}_{N-1}, x_2 \cdot \hat{x}_{N-1}, \ldots, x_{N-1} \cdot \hat{x}_{N-1}) + \mathbf{n}\end{aligned} \tag{1}$$

Here, $h = Ae^{j\theta}$ is a complex-valued, $\mathcal{CN}(0,1)$ distributed, fading coefficient. The components of the additive noise vector $\mathbf{n} = (n_0, n_1, n_2, \ldots, n_{N-1})$ are identically and independently distributed. Let each n_i be a circularly symmetric Gaussian random variable with variance $\sigma_n^2 = N_0/2$ per real dimension. Using the circular symmetry of the fading coefficient, we can rewrite (1) as

$$\begin{aligned}\mathbf{y} = (y_0, y_1, \ldots, y_{N-1}) &= h\hat{x}_{N-1}(1, x_1, x_2, \ldots, x_{N-1}) + \mathbf{n} \\ &= \tilde{h}(1, x_1, x_2, \ldots, x_{N-1}) + \mathbf{n}\end{aligned} \tag{2}$$

where $\tilde{h}$, defined by the product of the actual fading coefficient h by the last transmitted symbol from the previous block $\hat{x}_{N-1}$, has the same distribution as h. Therefore, we can think of $\tilde{h}$ as a virtual fading coefficient and treat the first component of each block as a pilot symbol. Since the blocks are overlapped, this encoding scheme provides a pilot symbol for each block without any overhead.

Given the received vector $\mathbf{y} = (y_0, y_1, \ldots, y_{N-1})$, the demodulator computes *a posteriori* probabilities (APP's) $P[x_i = u \,|\, \mathbf{y}]$, where u belongs to an MPSK signal constellation $\mathcal{S}$. This demodulator uses the phase quantization technique introduced in [5] to reduce the complexity of the standard noncoherent detector. We now illustrate computations done by the demodulator by computing $P[x_1 = u_1|\mathbf{y}]$. Let's assume that the phase $\theta \in [0, 2\pi]$ of the virtual fading coefficient $\tilde{h}$ is quantized into L discrete values

$$\theta \in \Phi = \{0, \frac{2\pi}{L}, 2\frac{2\pi}{L}, \cdots, (L-1)\frac{2\pi}{L}\}.$$

For the time being assume that the virtual fading amplitude A is known. Conditioned on the virtual fading amplitude A, the conditional *a posteriori* probability $P[x_1 = u_1|\mathbf{y}, A]$ can be written as follows:

$$\begin{aligned}&P[x_1 = u_1|\mathbf{y}, A] \\ &= \sum_{u_2} \cdots \sum_{u_{N-1}} P[x_0 = 1, x_1 = u_1, \ldots, x_{N-1} = u_{N-1}|\mathbf{y}, A] \\ &= C \cdot \sum_{u_2} \cdots \sum_{u_{N-1}} P[\mathbf{y}|x_0 = 1, x_1 = u_1, \ldots, x_{N-1} = u_{N-1}, A] \\ &\quad \cdot P[x_1 = u_1]P[x_2 = u_2] \cdots P[x_{N-1} = u_{N-1}],\end{aligned} \tag{3}$$

where C is a normalization constant. By introducing the quantization over θ and denoting $\theta_l = \frac{2\pi l}{L}$, we can rewrite (3) as

$$\begin{aligned}&P[x_1 = u_1|\mathbf{y}, A] \\ &= C_1 \cdot \\ &\sum_{l=0}^{L-1} \sum_{u_2} \cdots \sum_{u_{N-1}} P[\mathbf{y}|x_0 = 1, x_1 = u_1, \ldots, x_{N-1} = u_{N-1}, A, \theta_l] \\ &\qquad \cdot P[x_1 = u_1]P[x_2 = u_2] \cdots P[x_{N-1} = u_{N-1}] \\ &= C_2 \cdot \sum_{l=0}^{L-1} P[y_0|x_0 = 1, A, \theta_l]P[y_1|x_1 = u_1, A, \theta_l] \\ &\qquad \cdot \prod_{i=2}^{N-1} (\sum_{u_i} P[y_i|x_i = u_i, A, \theta_l]P[x_i = u_i]).\end{aligned} \tag{4}$$

Note that conditioned on the transmitted signal x_i, the fading amplitude A, and the fading phase θ_l, the received signal y_i is a complex Gaussian random variable with distribution $P[y_i|x_i, A, \theta_l] = \frac{1}{2\pi\sigma_n^2}\exp(-\frac{\|y_i - x_i A e^{j\theta_l}\|^2}{2\sigma_n^2})$.

In the case when the fading amplitude A is unknown, one can use a simple averaging estimator: $\hat{A}^2 = \frac{1}{N}\sum_{i=0}^{N-1}|y_i|^2 - 2\sigma_n^2$. It turns out that this simple estimator gives a satisfactory performance. For moderate coherence interval lengths, the use of this estimator will incur an extra $0.2 \sim 0.3$ dB performance degradation compared to the case when the fading amplitude is known.

D. *Joint Demodulation and Iterative Decoding*

In this paper, we use turbo codes and repeat-accumulate codes as examples of factor-graph codes that can be used on fading channels. In the following, we describe the joint demodulation and iterative decoding algorithm for these two classes of codes. For other factor-graph codes, an approach similar to one described here can be used.

Turbo Codes

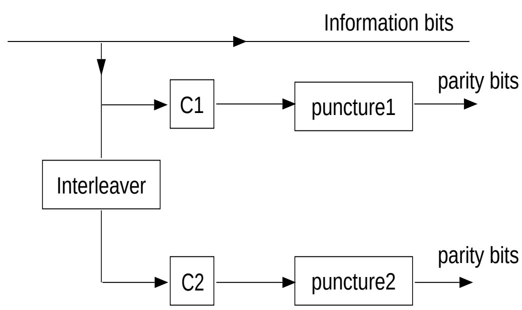

Figure 2: Encoder structure for turbo code

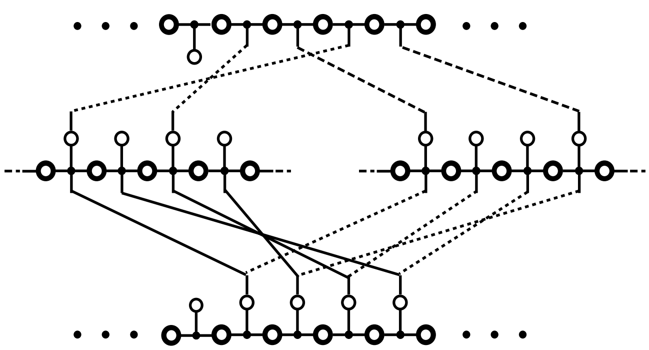

Figure 3: Factor-graph representation for joint demodulation and iterative decoding using turbo code

The joint demodulation and iterative decoding algorithm can be best explained with the help of a factor-graph that shows the flow of information as the algorithm proceeds iteratively. In this paper, we use the classical rate 1/2 turbo code proposed in [1] (see Figure 2). The corresponding factor-graph is shown in Figure 3. Two linear subgraphs at the center of the figure correspond to the constituent convolutional codes of the turbo code. The subgraphs on the top and the bottom represent blocks of parity symbols and information symbols respectively. We assume that information symbols and parity symbols are interleaved and sent over the channel separately, so that for a given block, the noncoherent demodulator processes either the information symbols or the parity symbols. In particular, top and bottom subgraphs in Figure 3 correspond to the block length of 5.

Information flow on the factor-graph is as follows: for each iteration, a block noncoherent demodulator computes APP's of the transmitted symbols using (4) and the *a priori* symbol probabilities $\{P[x_i = u_i] : i = 1, \ldots, N-1\}$ passed from the turbo decoder. The symbol APP's are used to compute APP's of the transmitted bits.

The APP's of the transmitted bits are deinterleaved and are passed to the turbo decoder. The turbo decoder works on the two center subgraphs. First, it runs a sum-product algorithm on the left subgraph and computes extrinsic information for the information bits and the first set of parity bits. Next, it runs a sum-product algorithm on the right subgraph and computes extrinsic information for the information bits and the second set of parity bits. Note that, in sum-product algorithm through each of these subgraphs, the turbo decoder computes the prior for information bits based on soft-information coming from the other subgraph and the noncoherent block demodulator.

Next, the turbo decoder computes *a priori* symbol probabilities $\{P[x_i = u_i] : i = 1, \ldots, N-1\}$ to be passed to the noncoherent block demodulator for the next iteration. It assumes that the bits that constitute a PSK symbol are independent of each other. Note that for information bits, there are two sets of extrinsic information, one from each center subgraph, available to the turbo decoder. In our implementation, the turbo decoder considers only the extrinsic information coming from the right subgraph. In this manner, the joint demodulation and iterative decoding proceeds iteratively.

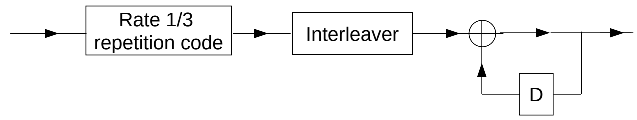

Figure 4: Encoder structure for repeat-accumulate code

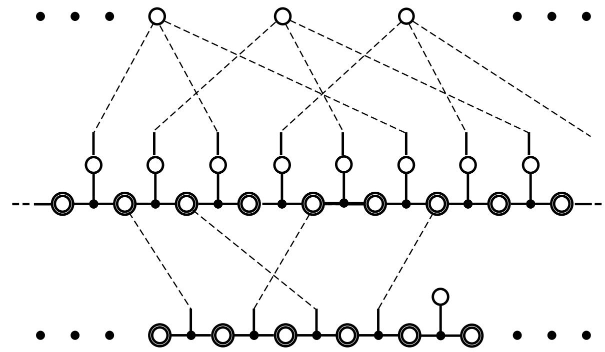

Figure 5: Factor-graph representation for joint demodulation and iterative decoding using repeat-accumulate code

Repeat-Accumulate Codes

Repeat-accumulate codes were first proposed in [8] as a class of turbo-like codes. The most distinguished feature of a repeat-accumulate code is that it has a very simple encoding structure consists of a repetition code and a rate 1 accumulator, as shown in Figure 4. Surprisingly, this simple code performs near channel capacity as well.

The joint demodulation and iterative decoding using repeat-accumulate codes is similar to that of turbo codes. The main differences come from the serially concatenated structure of repeat-accumulate codes. Figure 5 shows the factor-graph for joint demodulation and iterative decoding of a rate 1/3 repeat-accumulate code. For each iteration, information from the bottom subgraphs (representing the block differential encoder) is passed to the subgraph on the center. Next, a sum-product algorithm is run on the center subgraph (representing the accumulator) and the information is passed to the subgraph on the top (representing the repetition code). The information then flows back to the center subgraph before it is finally passed back to the bottom subgraph. Note that due to the simple constraints posed by the rate 1/3 repetition code the sum-product algorithm on the top subgraph has very low implementation complexity.

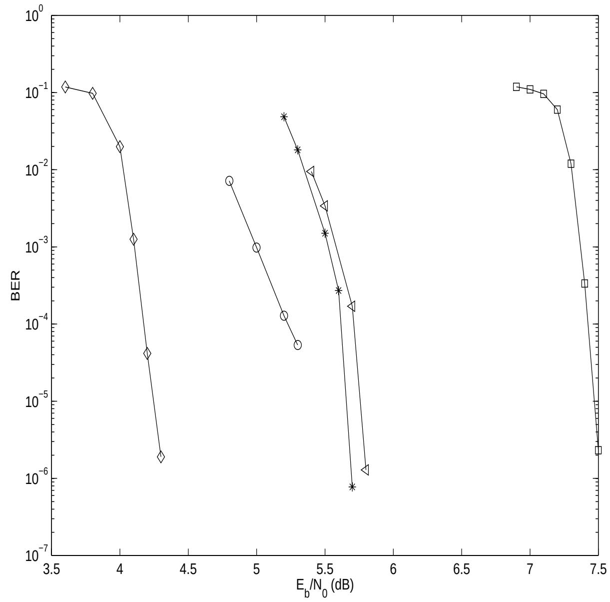

Figure 6: Performance of rate 1/2 turbo code for 8PSK modulation.

◇ coherent detection
▷ coherence interval 20 with unknown amplitude
∗ coherence interval 20 with known amplitude
○ coherence interval 100 with unknown amplitude
□ standard noncoherent DPSK

III. Simulation results

We extensively simulated the system shown in Figure 1 for 8PSK. We used a rate 1/2 turbo code with recursive systematic convolutional codes generated by the generators $(37/21)_8$. For all simulations, we chose interleaver length $2^{15} = 32768$, number of phase resolution $L = 80$, and 30 iterations of demodulation and decoding. Figure 6 shows the plots of bit error rate (BER) versus the ratio E_b/N_0, where E_b is the energy per information bit and N_0 is the one-sided power spectral density of the noise. The performance curve for coherently detected 8PSK is plotted to serve as a benchmark. At bit error rate 10^{-5}, this benchmark is within 1.0 dB of the minimum signal-to-noise ratio ($E_b/N_0 = 3.2$ dB) required to transmit 3/2 bits/sec/Hz.

Figure 6 also shows the performance of the joint demodulation and decoding algorithm proposed in this paper. For a coherence interval of length 20, the performance of the proposed algorithm is approximately 1.5 dB away from the coherent case. However, it is 1.7 dB better than the standard DPSK. Note that the performance of standard DPSK is about 3.2 dB away from the performance of the coherent PSK.

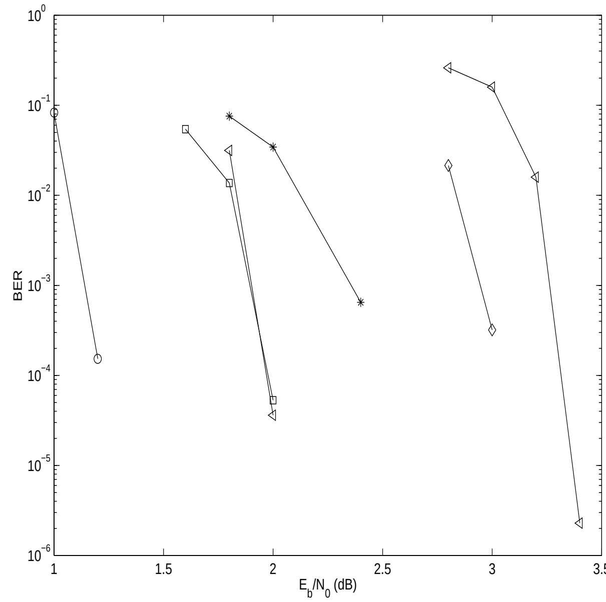

Figure 7: Performance of rate 1/3 repeat-accumulate code and rate 1/3 turbo code for BPSK modulation.

○ coherent detection for turbo code
□ coherent detection for repeat-accumulate code
◁ coherence interval 100 with unknown amplitude using turbo code
∗ coherence interval 100 with unknown amplitude using repeat-accumulate code
◇ coherence interval 20 with unknown amplitude using repeat-accumulate code
▷ coherence interval 20 with unknown amplitude using turbo code

Figure 7 shows the performance of a rate 1/3 repeat-accumulate code and the performance of a rate 1/3 turbo code for BPSK modulation. The rate 1/3 turbo code used in this paper shares the same parameters as described above for the rate 1/2 turbo code. Rate 1/3 is obtained by avoiding any puncturing. In this case, we chose number of phase resolution $L = 20$ and 40 iterations of demodulation and decoding. For coherent detection, repeat-accumulate code performs about 0.8 dB worse than the turbo code. However, for a coherence interval of moderate length 20, repeat-accumulate code outperforms turbo code by about 0.3 dB. As the length of the coherence interval increases, the turbo code overtakes the repeat-accumulate code. During our simulations, we observed that the joint demodulation and decoding algorithm for the repeat-accumulate code converges slower than that of the turbo code: the average number of iterations needed for the repeat-accumulate code is approximately twice as much as that of the turbo code. This slow convergence causes extrinsic information from the decoding algorithm to remain soft. On the other hand, for large coherence interval, block noncoherent demodulator takes less number of iterations to estimate the channel, that explains the better performance of turbo code at larger coherence interval.

As the coherence interval increases, the performance of the proposed noncoherent algorithm improves. This is in line with the capacity calculations in [5], which show that the potential penalty for noncoherent detection decreases as the length of the coherence interval increases. For example, when the length of the coherence interval is 100, the performance of the proposed noncoherent detector is within 1.2 dB of the coherent detector for the rate 1/2 turbo code and is within 0.8 dB for the rate 1/3 turbo code. Further improvements can be obtained by increasing the phase resolution level L and the length of the coherence interval N. However, the convergence to the coherent case for large coherence intervals appears to be quite slow, which is similar to conclusions reached from the information-theoretic analysis in [7].

IV. Conclusions

This paper proposes a joint demodulation and iterative decoding algorithm for factor-graph codes over noncoherent Rayleigh fading channels. Simulation results employing two factor-graph codes, turbo codes and repeat-accumulate codes, are presented. It was shown that as the length of the coherence interval increases, the performance of the proposed joint algorithm approaches that of the coherent detection. The proposed algorithm uses phase quantization and has a complexity which is linear in the length of the coherence interval.

Acknowledgments

The authors would like to thank Prof. Ralf Kötter for several stimulating discussions and suggesting the use of repeat accumulate codes.

References

[1] Berrou, C., A. Glavieux and P. Thitimajshima, "Near Shannon limit error-correcting coding and decoding: turbo codes," *Proceedings of the 1993 IEEE international Conference on Communication*, pp. 1064–1070, May 1993.

[2] Eric K. Hall and Stephen G. Wilson, "Design and Analysis of Turbo Codes on Rayleigh Fading Channels," *IEEE journal on selected areas in communications,* vol. 16, no. 2, pp. 160–174, February 1998.

[3] D. Divsalar and M.K. Simon, "Multiple-symbol differential detection of MPSK," *IEEE Trans. on Communications*, vol. 38, no.3, pp. 300–308, March 1990.

[4] M. Peleg and S. Shamai, "Iterative decoding of coded and interleaved noncoherent multiple symbol detected DPSK," *Electronics Letters*, vol. 33, no. 12, pp. 1018–1020, June 1997.

[5] Dilip Warrier and U. Madhow, "Noncoherent Communication in Space and Time," Preprint version, 1999.

[6] Giuseppe Caire, Giorgio Taricco and Ezio Biglieri, "Bit-Interleaved Coded Modulation," *IEEE Trans. on Information theory*, vol. 44, no.3, pp. 927–946, May 1998.

[7] Thomas L. Marzetta and Bertrand M. Hochwald, "Capacity of a Mobile Multiple-Antenna Communication Link in Rayleigh Flat Fading," *IEEE Trans. on Information Theory*, vol. 45, no. 1, pp. 139–157, January 1999.

[8] D. Divsalar, H. Jin, R. J. McEliece, "Coding Theorems for "Turbo-like" Codes", *Proceedings on the Thirty-Sixth Annual Allerton Conference on Communication, Control, and Computing,*, pp. 201–210, 1998.

[9] M. Peleg, S. Shamai(Shitz), and S. Galán, "On iterative decoding for coded noncoherent MPSK communications over block-noncoherent AWGN channel", *Proc. Int. Conf. Telecommunication, ICT'98*, pp. 109–114, 1998.

[10] P. Hoeher, J. Lodge, "Turbo DPSK: Iterative differential PSK demodulation and channel decoding," *IEEE trans. on communications*, vol. 47, no.6, pp. 837–843, June 1999.